

Measuring Potassium Polarization with Optical  
Probing of  $4s_{\frac{1}{2}} \rightarrow 5p_{\frac{1}{2}}$  Hyperfine Transitions

Dante Prins With Dr. John Behr

September-December 2021

# Contents

<b>1</b>	<b>Introduction</b>	<b>3</b>
<b>2</b>	<b>Zeeman Splitting Energies and the Breit-Rabi formula</b>	<b>3</b>
<b>3</b>	<b>Saturation Spectroscopy</b>	<b>6</b>
<b>4</b>	<b>Optical Probing Measurements</b>	<b>7</b>
4.1	F=2 data . . . . .	9
4.2	F=1 data . . . . .	13
4.3	nuclear polarization calculations . . . . .	19
<b>5</b>	<b>Practical Notes and Future Improvements</b>	<b>19</b>
5.1	DLC pro tips and tricks . . . . .	19
5.1.1	Outputting scan voltage . . . . .	20
5.1.2	feed forward coefficient . . . . .	20
5.1.3	DLC Pro screenshots . . . . .	20
5.1.4	DLC Pro PC software . . . . .	21
5.1.5	startup procedure . . . . .	21
5.1.6	locking the laser on the DLC Pro box . . . . .	21
5.2	optical pumping simulation in python . . . . .	22
5.2.1	pumping power . . . . .	22
5.2.2	stimulated emission and excitation losses . . . . .	22
5.2.3	pump detuning and power broadening . . . . .	23
5.2.4	$\pi$ light probing . . . . .	23
5.2.5	Larmor precession . . . . .	23
5.3	possible wave plate burying . . . . .	23
5.4	laser mode hopping prevention . . . . .	23
5.5	AOM scanning power shifts . . . . .	23
5.6	power broadening . . . . .	24
<b>6</b>	<b>Bibliography</b>	<b>24</b>

## 1 Introduction

This report is a summary of the work and findings of my four-month CO-OP work placement at TRIUMF in 2021. Please send me an email at dantemprins@gmail.com if you have any questions. The goal of my appointment was to configure and lock a newly purchased 405nm tunable diode laser, and use it to perform a measurement of the polarization of potassium-41 in the trap by probing the  $D_1$ -line:  $4S_{\frac{1}{2}} \rightarrow 5P_{\frac{1}{2}}$  transitions. Ultimately this setup will be used for other measurements, including imminently the  $D_2$ -line:  $4S_{\frac{1}{2}} \rightarrow 5P_{\frac{3}{2}}$  transitions.

## 2 Zeeman Splitting Energies and the Breit-Rabi formula

In the absence of a magnetic field, Hyperfine Structure is observed from the interaction between the orientation of the nuclear dipole moment relative to the total momentum of the valence electron. This yields energy splitting:

$$E_{HFS} = A \langle I \cdot J \rangle = \frac{A}{2} F(F+1) - I(I+1) - J(J+1) \quad (1)$$

for different quantum numbers and degeneracy of  $2 * F + 1$ . Where for  $K_{41}$ :

Fine Structure	A coefficient (MHz)
$4s_{\frac{1}{2}}$	126.9
$5p_{\frac{1}{2}}$	4.97

The Zeeman effect appears when one introduces a magnetic field which interacts with the nuclear and electron dipole. Combining this effect with the hyperfine structure above, it yields a Hamiltonian:

$$H = A \vec{I} \cdot \vec{J} - (\mu_N g_I \vec{I} + \mu_B g_J \vec{J}) \cdot \vec{B}. \quad (2)$$

Recall the  $|F, m_F\rangle$  basis is conventional for hyperfine states, however the Hamiltonian is described in  $|m_I, m_J\rangle$ . For  $J = \frac{1}{2}$ , as is the  $5P_{\frac{1}{2}}$  and  $4S_{\frac{1}{2}}$  cases, each hyperfine state  $|F, m_F\rangle$  is a linear combination of two states in the  $|m_I, m_J\rangle$  basis, leading to a two state degenerate perturbation system for each  $|F, m_F\rangle$  state.

For the definitions  $|F, m_F\rangle = \alpha |+\rangle + \beta |-\rangle$ ,  $|\pm\rangle = |m_J = \pm \frac{1}{2}, m_I = m_F \mp \frac{1}{2}\rangle$ , through ladder operations on the Hamiltonian [1] we get

$$H = \begin{pmatrix} -\frac{A}{4} + \mu_N g_I m_F B + \frac{1}{2}(A m_F + \mu_B g_J - B \mu_N g_I) & \frac{1}{2} A \sqrt{(I + \frac{1}{2})^2 - m_F^2} \\ \frac{1}{2} A \sqrt{(I + \frac{1}{2})^2 - m_F^2} & -\frac{A}{4} + \mu_N g_I m_F B - \frac{1}{2}(A m_F + \mu_B g_J - B \mu_N g_I) \end{pmatrix} \quad (3)$$

The positive eigenenergy is defined as  $F = 2$  while the negative  $F = 1$ .

$$\Delta E_{F=2} = -\frac{A}{4} + \mu_N g_I m_F B + A \sqrt{1 + m_F x + x^2}, \quad (4)$$

$$\Delta E_{F=1} = -\frac{A}{4} + \mu_N g_I m_F B - A \sqrt{1 + m_F x + x^2} \quad (5)$$

Where  $x = \frac{B(\mu_B g_J - \mu_N g_I)}{2A}$ .

Below is an example of how the energies behave for the eight hyperfines of  $5P_{\frac{1}{2}}$ .

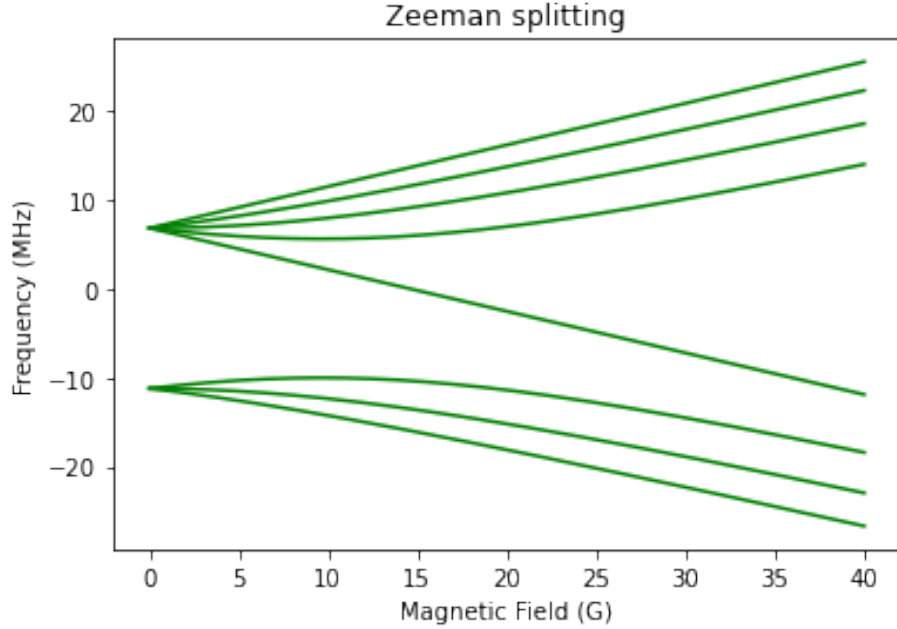


Figure 1: Zeeman splitting of the  $K_{41}5P_{\frac{1}{2}}$  hyperfines.

Eigenstates found are then

$$|F = 2, m_F\rangle = \alpha |+\rangle + \beta |-\rangle, |F = 1, m_F\rangle = \beta |+\rangle + \alpha |-\rangle \quad (6)$$

where

$$\alpha^2 = \frac{1}{2} + \frac{A m_F + B \mu_B g_J - B \mu_N g_I}{4A \sqrt{1 + m_F x + x^2}}, \beta^2 = \frac{1}{2} - \frac{A m_F + B \mu_B g_J - B \mu_N g_I}{4A \sqrt{1 + m_F x + x^2}} \quad (7)$$

Notice we recover the Clebsch-Gordan Coefficients at  $B = 0$  and that at  $B \rightarrow \infty$  we reach pure states, namely  $|F = 2, m_F\rangle = |+\rangle$  and  $|F = 1, m_F\rangle = |-\rangle$ .

For  $m_F = \pm 2$  the states are already pure at  $B = 0$  and the Hamiltonian reduces to single state solutions where  

$$\Delta E_{F=2} = \frac{A_3}{4} + \mu_N g_I m_F B$$

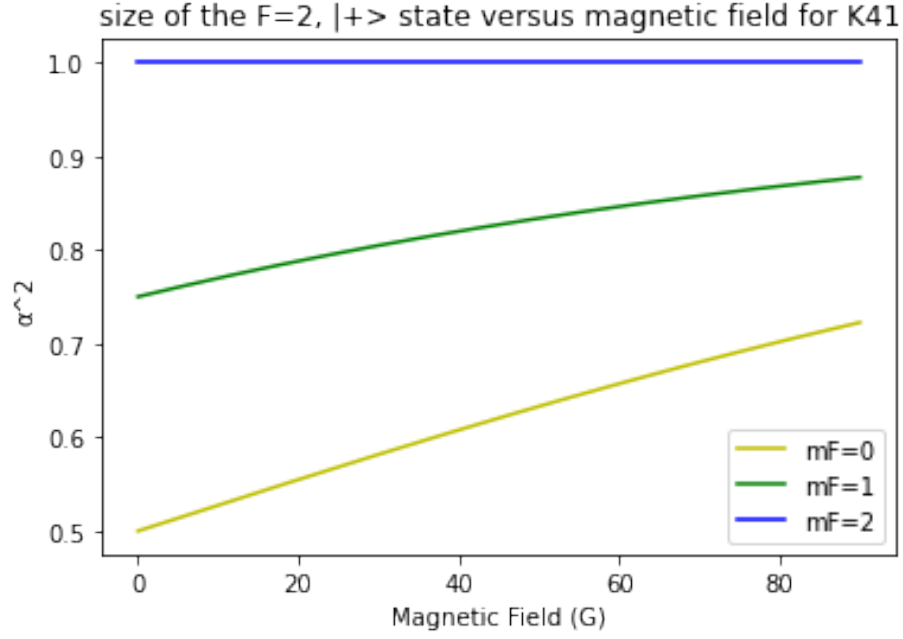


Figure 2: plot of the coefficient  $\beta^2$  from  $|F = 2, m_F\rangle = \alpha |+\rangle + \beta |-\rangle$  as a function of magnetic field. Note that  $\beta^2 = 1 - \alpha^2$ .

### 3 Saturation Spectroscopy

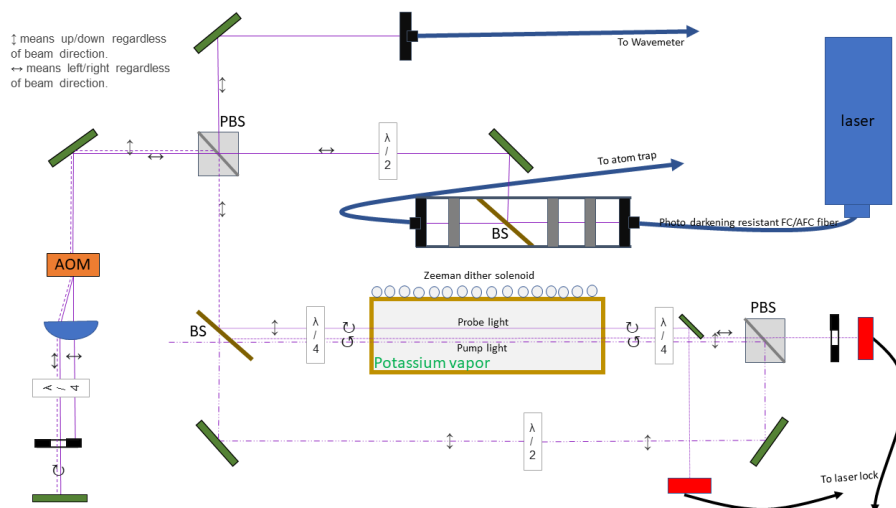


Figure 3: The optical setup used split light to the trap, lock the 405nm laser and display wavelength on a Wavemeter for characterization.

Beginning at the laser head, the fiberdock was tuned to maximum at low power(45mA) to prevent any damage. The included 'Longlife' photo darkening protected fiber is specified as FC/AFC, all other connectors used are in the FC/APC form. This included the input to the telescope, however we found than a FC/APC collimator fit okay with a FC/AFC fiber. For more information on these connectors please read [https://www.ozoptics.com/ALLNEW\\_PDF/APN0006.pdf](https://www.ozoptics.com/ALLNEW_PDF/APN0006.pdf).

The telescope was designed with two similar collimators with a focal in the center. A 90/10 beam splitter presently diverts most of the light towards the optics table, while the rest is sent to the atom trap. Hopefully the fibercoupler ordered will replace this in the new year. The leading  $\frac{\lambda}{2}$  waveplate is used to control the ratio of light split between the Wavemeter and potassium cell for Saturation Spectroscopy by changing the linear polarization direction for the upcoming polarizing beamsplitter which deflects  $\uparrow$  upwards while  $\leftrightarrow$  light passes through.

Concerning the Wavemeter beam, we have observed optical feedback effects, so it would be prudent to either block this path or verify it's blocking does not affect the satSpec signal when an accurate signal is needed.

The  $\leftrightarrow$  beam passes through the PBS and travels through the AOM and back to be frequency shifted and rotated to  $\uparrow$  light that is then deflected downwards by the PBS towards the trap. The Acoustic Optical Modulator shifts light by it's acoustic frequency and with two passes we can double that effect. Please note we have noticed a efficiency dependence of the AOM on shifting frequency

this could be as much as 50% of the first order beam intensity for  $20MHz$  of shifting.

The shifted light travels down to the heated potassium cell where a small percentage is split right as two probe beams of equal intensity. The rest travels around the cell to enter via the opposite direction and is dubbed the pump beam.

Please note the  $\frac{\lambda}{2}$  waveplate on the pump line must be thought of as an attenuator exploiting the PBS, not as an optimization tool; removing the component should result in full power being deflected at the PBS. At one point in the term, another  $\frac{\lambda}{2}$  waveplate was placed before the satSpec beams split, meaning to manipulate the polarization dependence of the beam splitter for more power in the probes. However, this caused the pump and probe beams to be mispolarized relative to each other in the trap because of the absolute effect of the downstream PBS.

For this setup to work, we rely on the incoming and outgoing beams outside the  $\frac{\lambda}{4}$  plates to be  $\frac{\pi}{2}$  out of phase and vice-versa for the pump beam. Adding another wave plate violated this and at that time our setup had necessarily imperfect pump or probe light in terms of being circularly polarized.

The pump beam was usually aligned with the lower probe beam through the cell. The lower beam is then read by a photo diode and is used to lock the laser. The upper probe beam was deflected downwards and subtracted from the first probe to produce a signal only comprised of satSpec effects and subtract other fluctuations.

An additional tool is to place another photo diode behind the BS to measure the power of the pump beam after it has passed through to get a rough measurement of AOM efficiency and other effects that change general beam power.

## 4 Optical Probing Measurements

Scans of K41 spectra were performed in the atom trap to determine the degree of optical polarization that was achieved in the trap.

Via the double-pass  $150MHz$  AOM, the K39 lock was shifted to target the K41 spectra which has a  $455.9MHz$  isotope shift.

To target the transitions from the  $F = 2$  ground, the laser was locked at  $55.5MHz$ , the middle peak of the center family(crossovers). The AOM was then scanned between  $143.84MHz - 163.99MHz$ , hitting the trap at  $343.2MHz - 383.5MHz$ .

To target the transitions from the  $F = 1$  ground, the laser was locked at  $295.3MHz$ , the right peak of the right family( $4s_{\frac{1}{2}}F = 1 \rightarrow 5p_{\frac{1}{2}}F = 2$ ). The AOM was then scanned between  $152.5MHz - 172.5MHz$ , hitting the trap at  $600.3MHz - 640.3MHz$ .

Transitions for K41:

Ground State	Excited State	Frequency Shift (MHz)
$F = 2$	$F = 1$	354.43
$F = 2$	$F = 2$	364.37
$F = 1$	$F = 1$	608.45
$F = 1$	$F = 2$	618.39

Our 405nm laser produced  $\pi$  light to scan the  $4s_{1/2} \rightarrow 5p_{1/2}$  405nm transition to probe the polarization of the ground state K41 atoms. The experiment was performed with alternating Optical Probing light and Magnetic Optical Trapping light. Triggering on the duty cycle produces the OP+ scans, the beam polarization was flipped to produce the OP- scan. collecting all counts from the trap yields the All scan which has both OP+ and MOT counts. By subtracting OP+ from All we get the MOT counts.

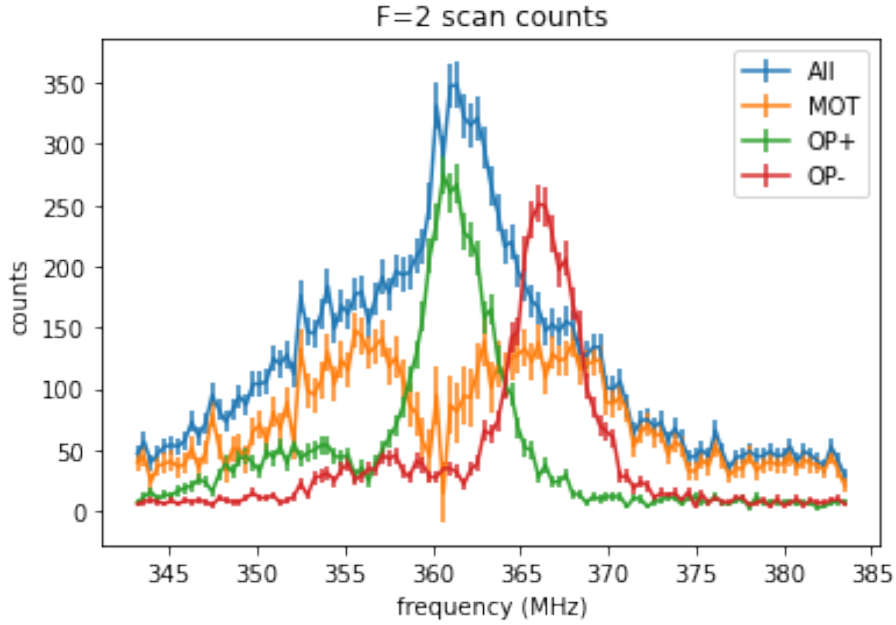


Figure 4: Electron detector events for the three scans performed on the F=2 ground state transitions.

These scan can then be fitted to the seven and five respective allowed transitions for the F=2 and F=1 ground states to determine polarization.

The fit parameters were magnetic field,  $\sigma$  and  $\gamma$  coefficients of the transition Voigt profiles and the hyperfine polarization populations:  $[-2, -1, 0, 1, 2]$  for F=2,  $[-1, 0, 1]$  for F=1. The Voigt profiles themselves were functions of B, as the Zeeman Splitting in equation 4 and 5 was used to calculate the resonance of each transition within the fit.



## 4.1 F=2 data

An initial fit of the MOT data produced:

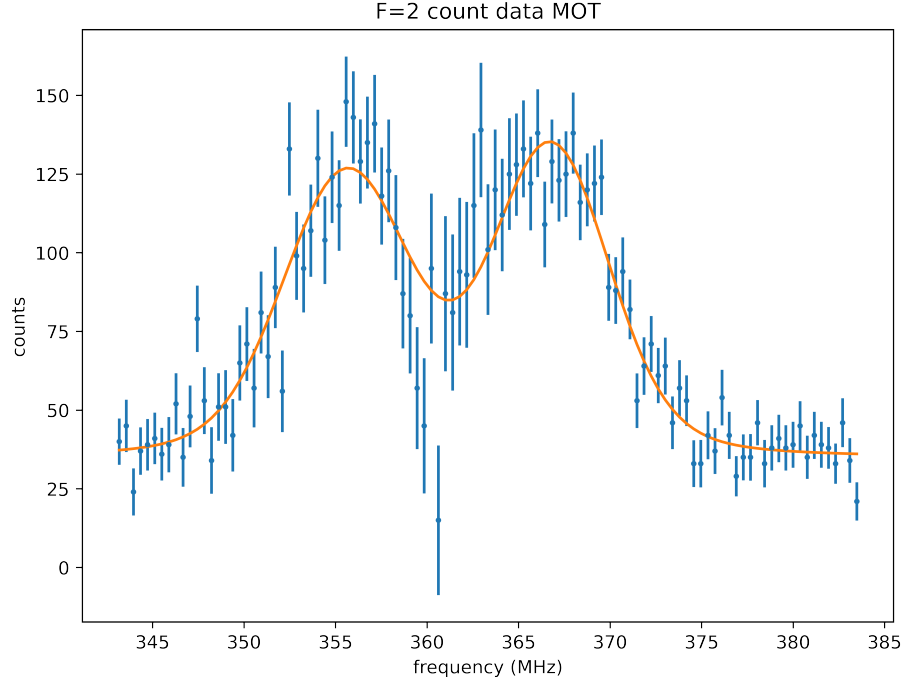


Figure 5: F=2 uncorrected electron event counts for the MOT portion of the duty cycle.

Fit parameter	Value	Value error (1SD)
$m_F = 2$ relative population	$4e - 15$	78.6
$m_F = 1$ relative population	$2.9e - 17$	41.5
$m_F = 0$ relative population	105.3	79.0
$m_F = -1$ relative population	146.4	96.9
$m_F = -2$ relative population	182.0	41.5
Magnetic field	2.688G	0.80G
$\sigma$	2.78MHz	1.09MHz
$\gamma$	0.90MHz	1.48MHz

clearly we have over subtracted the OP+ signal to extinguish all positive polarization population. Adding the coefficient 0.6 to OP+ balances the populations. It was observed the laser could have fallen out of lock during the All scan, leading to lower population counts. Different behavior in the trap between the two scans is also possible.

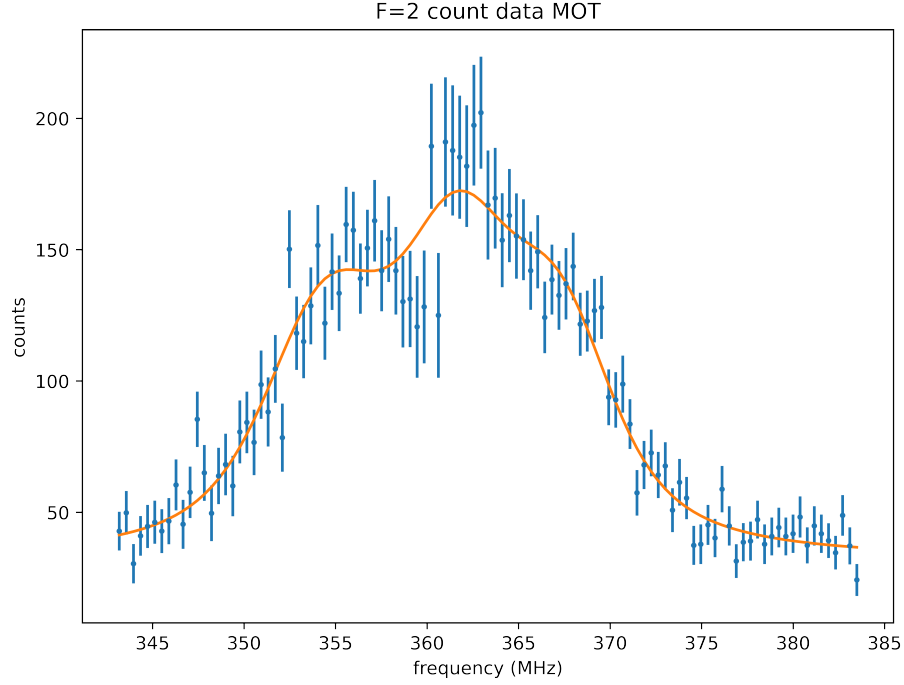


Figure 6:  $F=2$  corrected electron event counts for the MOT portion of the duty cycle.

Fit parameter	Value	Value error (1SD)
$m_F = 2$ relative population	247.4	43.6
$m_F = 1$ relative population	26.6	36.5
$m_F = 0$ relative population	171.3	55.1
$m_F = -1$ relative population	73.7	64.9
$m_F = -2$ relative population	180	20.8
Magnetic field	$3.02G$	$0.80G$
$\sigma$	$1.72MHz$	$0.83MHz$
$\gamma$	$2.41MHz$	$0.95MHz$

These corrected numbers seem more reasonable.

This analysis is less important for a final measurement, now we fit to OP+ and OP- measurements to determine the quality of polarization achieved in the trap.

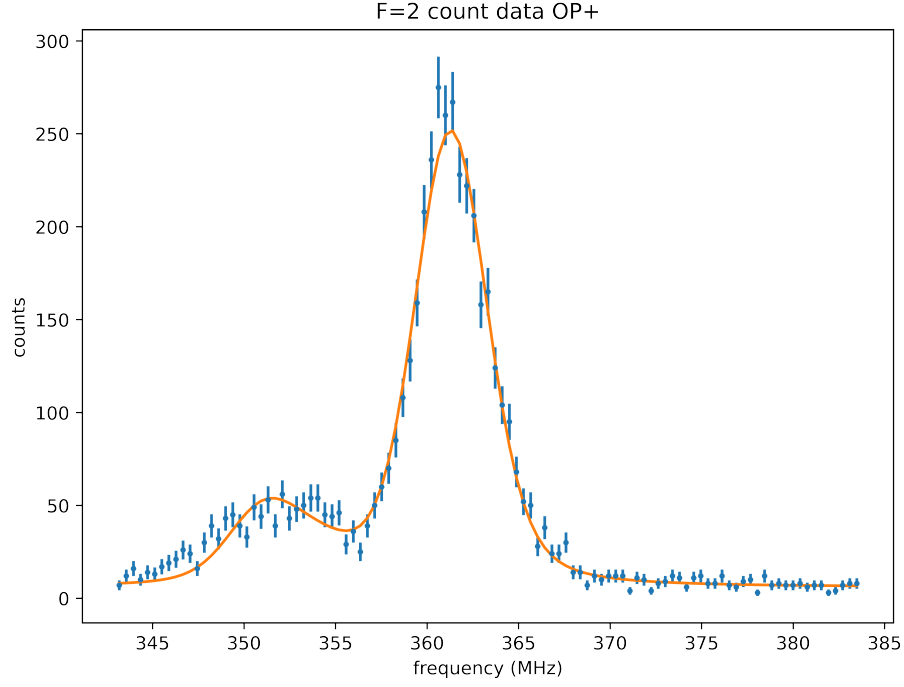


Figure 7: F=2 electron event counts for the OP+ scan.

Fit parameter	Value	Value error (1SD)
$m_F = 2$ relative population	333.3	1.13
$m_F = 1$ relative population	73.4	33.5
$m_F = 0$ relative population	21.5	7.7
$m_F = -1$ relative population	$1.9e - 12$	8.0
$m_F = -2$ relative population	$9.3e - 11$	20.6
Magnetic field	$3.43G$	$0.08G$
$\sigma$	$1.64MHz$	$0.24MHz$
$\gamma$	$0.72MHz$	$0.42MHz$

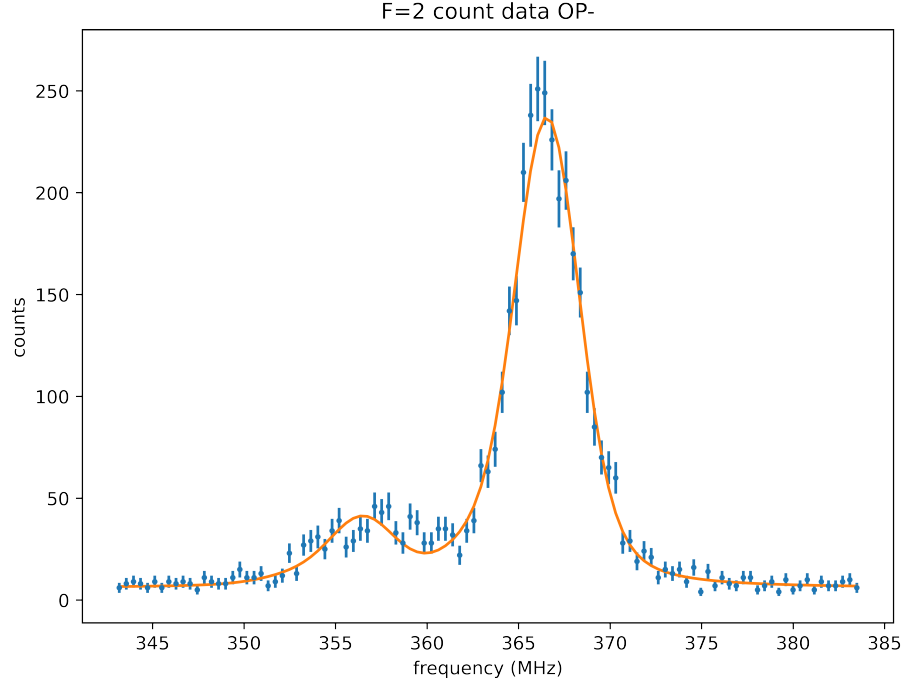


Figure 8: F=2 electron event counts for the OP- scan.

Fit parameter	Value	Value error (1SD)
$m_F = 2$ relative population	10.0	4.6
$m_F = 1$ relative population	3.6	6.2
$m_F = 0$ relative population	3.9	7.1
$m_F = -1$ relative population	53.0	11.8
$m_F = -2$ relative population	287.2	0.8
Magnetic field	2.29G	0.06G
$\sigma$	1.47MHz	0.13MHz
$\gamma$	0.70MHz	0.16MHz

Combining these five populations with the three populations from the F1 fits will yield our system polarization.

## 4.2 F=1 data

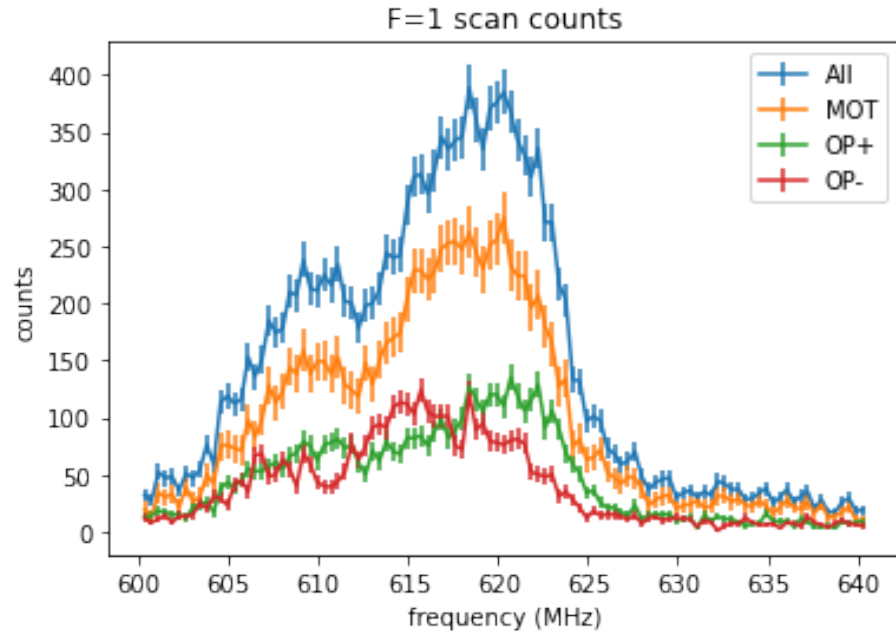


Figure 9: Electron detector events for the three scans performed on the F=1 ground state transitions.

First the MOT was fit:

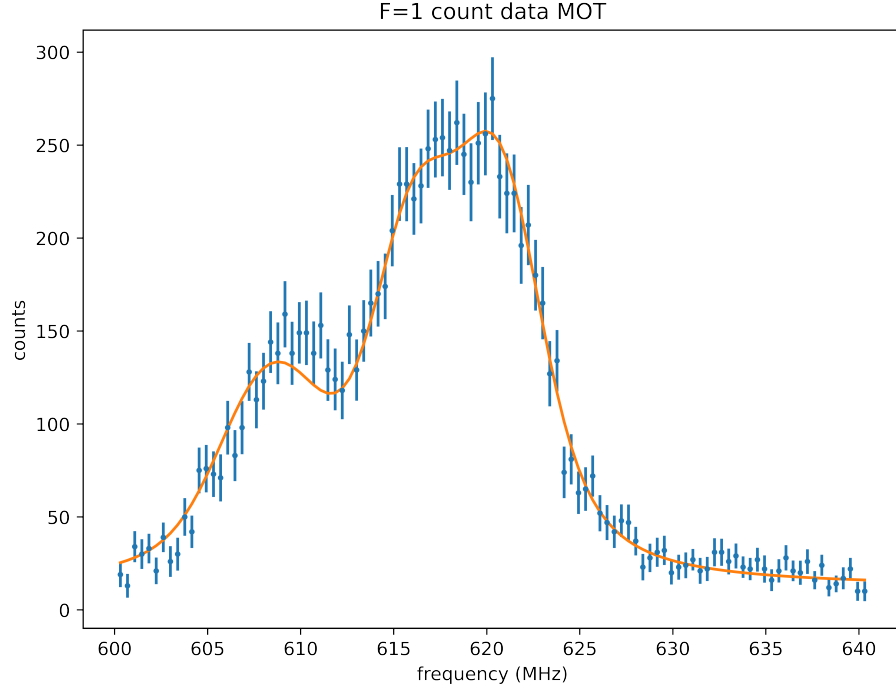


Figure 10:  $F=1$  electron event counts for the MOT portion of the duty cycle.

Fit parameter	Value	Value error (1SD)
$m_F = 1$ relative population	486.7	30.6
$m_F = 0$ relative population	28.1	31.3
$m_F = -1$ relative population	407.8	20.5
Magnetic field	$2.53G$	$0.13G$
$\sigma$	$1.56MHz$	$0.27MHz$
$\gamma$	$1.62MHz$	$0.30MHz$

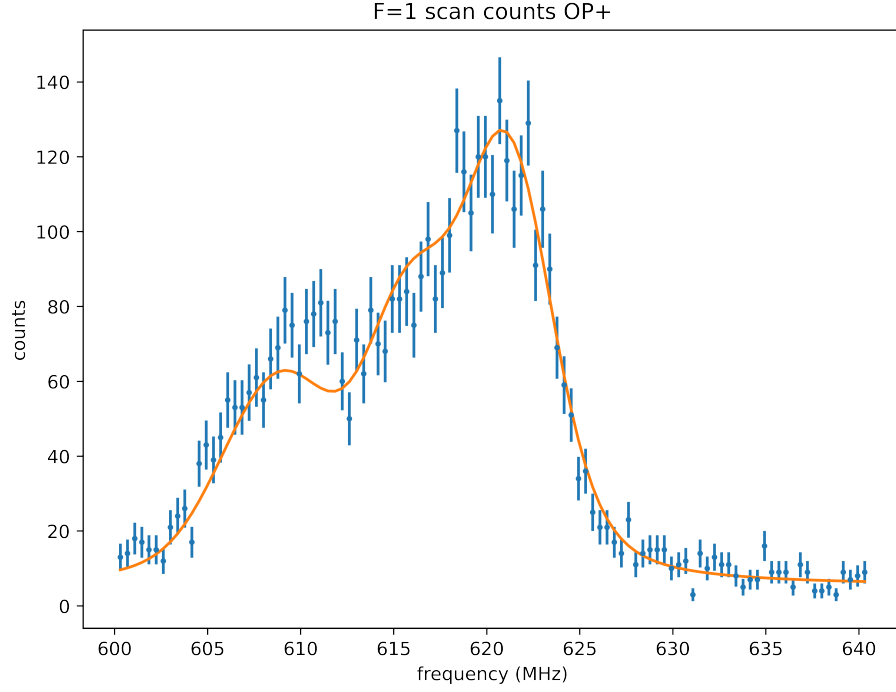


Figure 11: F=1 electron event counts for the OP+ scan.

Fit parameter	Value	Value error (1SD)
$m_F = 1$ relative population	265.6	20.1
$m_F = 0$ relative population	$6.6e - 16$	18.2
$m_F = -1$ relative population	157.7	10.7
Magnetic field	$2.90G$	$0.15G$
$\sigma$	$1.97MHz$	$0.27MHz$
$\gamma$	$1.04MHz$	$0.36MHz$

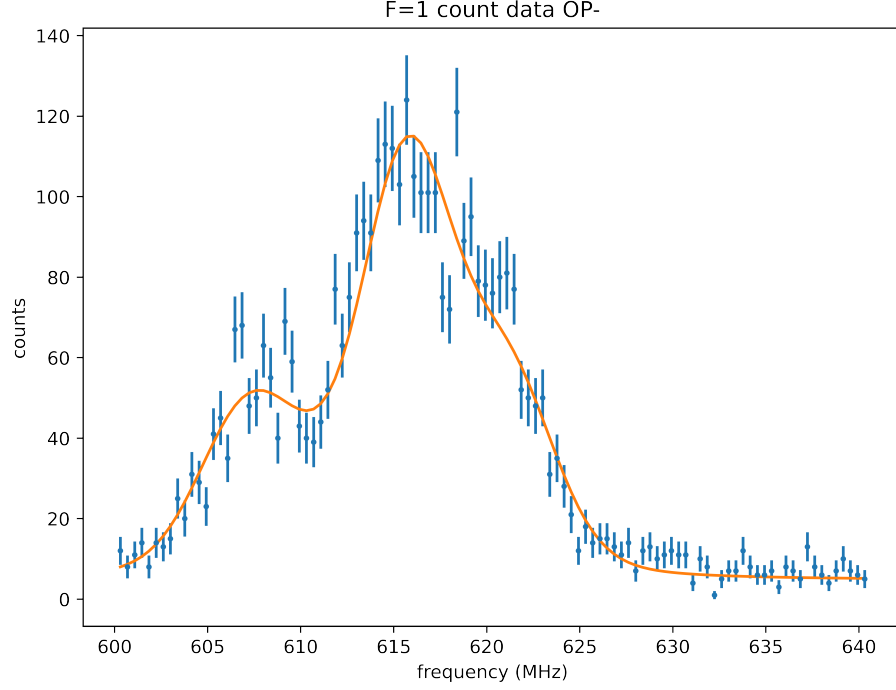


Figure 12: F=1 electron event counts for the OP- scan.

Fit parameter	Value	Value error (1SD)
$m_F = 1$ relative population	106.3	12.9
$m_F = 0$ relative population	$3.12e - 15$	19.5
$m_F = -1$ relative population	236.7	17.7
Magnetic field	$2.95G$	$0.20G$
$\sigma$	$2.26MHz$	$0.35MHz$
$\gamma$	$0.61MHz$	$0.56MHz$

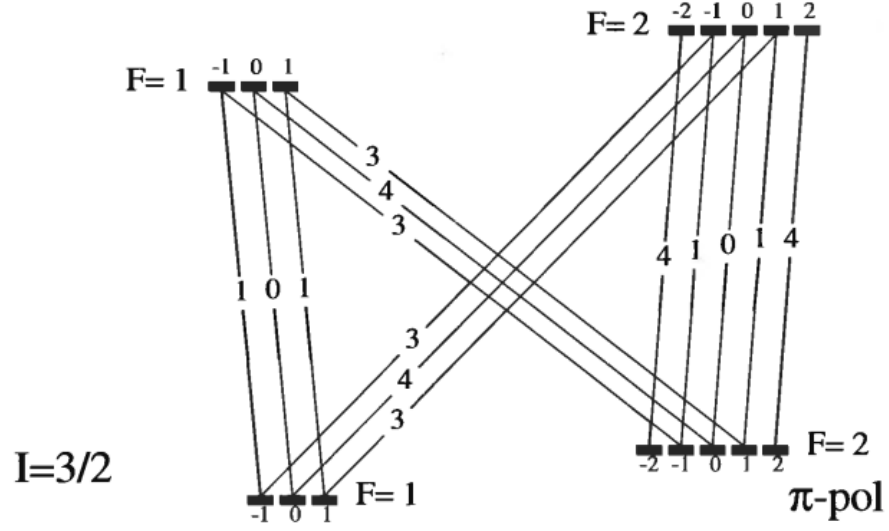
Already we see clear flaws in the fits with the  $m_f = 1$  populations being zero with no clear physical explanation being present. Because the  $1 \rightarrow 1, m_f = 0$  transition is forbidden, it is clear the fit sees the ratio between the left and right peaks above the theoretical maximum of 1:3 (see D1  $\pi$  line in figure 13 below), and is trying to minimize this discrepancy. This can also be seen by the consistent under fitting of the left peak.

This could be explained by many factors, including the laser power on the lock changing. The AOM was observed to behave more efficiently at one end of the frequency scan, with power dipping as low as 1/2 on the other. As we were not able to produce a true zero-crossing lock in the signal, this leads to a frequency dip in laser lock as the PID will move up and down the zero-crossing signal to track a shifting zero. This could cause scans to be compressed



or stretched in frequency on one end, causing the left peak to appear larger because of an x-axis shift. A fit parameter to account for x-axis stretching was attempted but did not effectively fix this discrepancy.

D<sub>1</sub>-line:  $^2S_{1/2}-^2P_{1/2}$



D<sub>1</sub>-line:  $^2S_{1/2}-^2P_{1/2}$

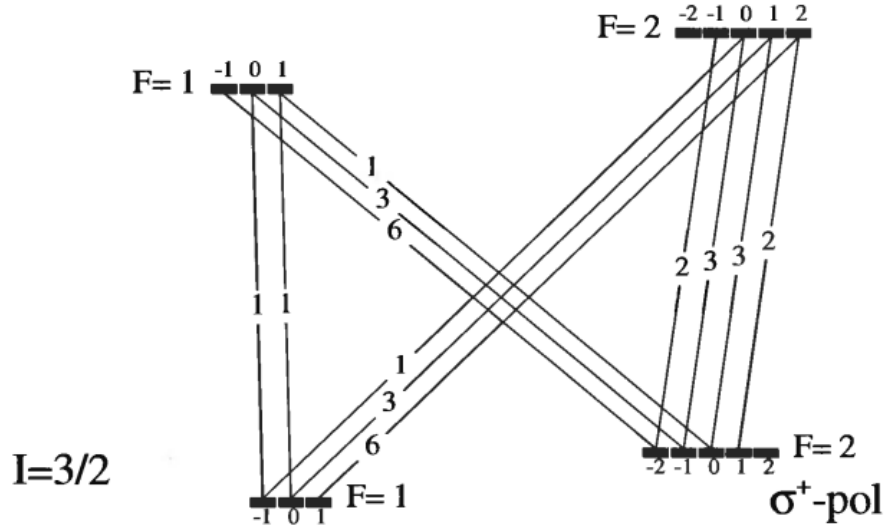


Figure 13: Transition strengths of hyperfine states in an  $I = 3/2$  atom, from Metcalf's Laser Cooling and Trapping pg 284.

### 4.3 nuclear polarization calculations

The nuclear polarization can now be calculated from the relative populations of each fit. Because scans were done for the same amount of time and only one day apart, we have assumed there is parity between the count rates from the F=1 and F=2 data, that is to say the other spectra would reproduce when the first was detected and vice-versa. This assumption could be avoided by using the MOT scans to determine a normalization coefficient between the scans by assuming at rest the system will behave in a 3:5, F1:F2 ratio. These steps have not been taken because both the MOT scans have clear issues reporting what should be the same population for each of the transitions.

To calculate precise relations between the  $|F, m_f\rangle$  and  $|m_I, m_J\rangle$  basis we use equation 6 as a function of magnetic field. That being said, to simplify error propagation we will compute the mean between the  $F_1, F_2$  magnetic fields and take this as a known parameter. This simplification should be negligible because the magnetic field is very small as to only slightly perturb the populations from the default Clebsch-Gordon coefficients.

$$B_{OP+} = 3.31G \quad B_{OP-} = 2.34G$$

The equation for nuclear polarization is:

$$P = \frac{\langle \vec{I} \rangle}{I} = \sum \frac{p_{F, m_f}}{I} * \langle F, m_f | m_I | F, m_f \rangle = \sum \frac{p_{F, m_f}}{I} (\alpha^2(m_f - \frac{1}{2}) + \beta^2(m_f + \frac{1}{2})) \quad (8)$$

Where  $p_{F, m_f}$  are the calculated populations normalized.

The error of a function in the form  $f(x) = \frac{x_1 c_1 + x_2 c_2 \dots}{x_1 + x_2 \dots}$  with  $n$  measurements is:

$$\delta f(x) = \sum \left| \frac{c_n}{x_1 + x_2 \dots} - \frac{x_1 + x_2 \dots}{(x_1 + x_2 \dots)^2} \right| * \delta x_n \quad (9)$$

Using equations 8 and 9 we calculate the nuclear polarization as:

$$P_{OP+} = 0.541 \pm 0.066$$

$$P_{OP-} = 0.601 \pm 0.086$$

Treating these as one observable we get  $P = 0.563 \pm 0.021$ .

## 5 Practical Notes and Future Improvements

### 5.1 DLC pro tips and tricks

Please note I wrote all of these tips when we had the lock option trial and all the locking was done on the DLC pro box. Some of this may not apply to you.

### 5.1.1 Outputting scan voltage

If you desire to read the voltage scan on an external scope the piezo voltage of the DLC must be outputted, which is not directly available. Voltage scan can be viewed on external scope by connecting an input and output channel on the DLC and setting the piezo voltage as external and setting the scan parameter to an external channel. Now you are scanning externally to a channel which controls piezo voltage but can be Teed to the scope.

The voltage offset can create confusing effects with an external lock, I would recommend zeroing this and using the Classic Controller menu to adjust the voltage directly as this will not effect the outputted signal.

### 5.1.2 feed forward coefficient

Feed forward exists to modulate current with voltage so that a single mode can be maintained while the scope is scanned. Feed forward coefficient provided by the manufacturer as  $-1.28\text{mA/V}$ . This was done for a different mode than the one being used. A fit was performed on day-to-day found resonances near  $110\text{mA}$ , with a slope of  $-0.3\text{mA/V}$ . No such linearity was found at the  $120\text{mA}/50\text{V}$  mode where resonance may also be.

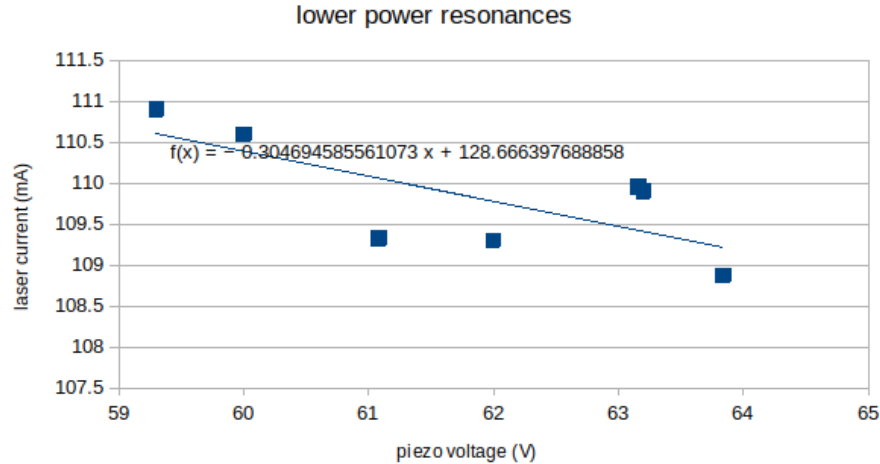


Figure 14: Fit of the laser current and voltages where resonance was found.

From this graph it's possible to recommend a feed forward of  $-0.3\text{mA/V}$  but from experience it's still unclear what the correct value should be.

### 5.1.3 DLC Pro screenshots

If a stick is placed in the front of the system screenshots can be taken by holding the disk button through two chimes/6 seconds.

#### 5.1.4 DLC Pro PC software

As an addition to the touchscreen controller, the system has a USB output on the rear which can be connect to DLC pro computer software. The computer software provided was not very helpful for me, the scope updated less than 1hz. This could be due to hardware limitations with a small laptop or serial limitations. Be aware connecting the software can reset DLC parameters some of which are less obvious than simply changing voltage to take you off resonance. My primary interest in the software was to use the PID optimization feature, However the lock wizard changes parameters that mean you have to find the resonance inside the wizard, and the resonances were not detected automatically(graphicly circled) by software so no lock could be made with the wizard. For this purpose my opinion is the software is not worth using. I did not investigate whether it was effective to export data and instead outputted the piezo voltage to recreate the onscreen scan.

#### 5.1.5 startup procedure

The satSpec cell needs a minimum of one hour before it's worth looking for absorption, it could be longer in my experience. The laser manual says it will stabilize thermally in a few minutes, I am inclined to believe it from observed behavior. The time period for the AOM to hit thermal equilibrium in the present setup is not clear but I would guess under twenty minutes. Once everything is warm you should look for the desired frequency on the wavemeter, and look at it's interferometry output to determine if the beam is single mode(smooth shapes as opposed to jagged). On the wave meter JR system I have observed the read frequency to be off by  $1\text{cm}^{-1}$  so it could read 0-1, 1-2 or 2-3 at a mode of 1.4 (all plus  $24700\text{cm}^{-1}$  of course). Once you are on the right mode, turn on the scan and search for resonance by changing the scan amplitude and the center piezo voltage. Mode hops should be obvious from the wavemeter interferometry output, you can adjust the current to avoid them, or turn off the feed forward and recenter the voltage. One trick is to look at the DLC pro lockin signal and let the system detect the resonance for you. This was very successful for me on noisy signals.

#### 5.1.6 locking the laser on the DLC Pro box

Because the software did not automatically determine lock candidates, make sure to set 'lock without lockpoint', the laser will try to zero to the height you set the lockpoint. PID will have to manually set without the lock wizard. The PID has two heads, PID1 for fast frequency with current changes and PID2 for low frequency with voltage changes. I used multiple methods, including Ziegler-Nichols, the one described by Toptica in the manual and what my own intuition was from building a tape following robot. All three of these converged on similar numbers, Toptica might have done the best. Reiterating the manual you should turn off PID1 and tune PID2 before optimizing with PID1.

PID1		PID2	
'Tape follower's intuition'			
P=2	I=2	P=1	I=1
G=8.24	D=10	G=0.2	D=0
Toptica			
P=2.3	I=5.6	P=1.4	I=7.8
G=6	D=10	G=0.2	D=4.8
Ziegler-Nichols			
*	*	P=0.3	I=2
*	*	G=0.2	D=25

Figure 15: The final numbers for various PID tuning methods on the DLC Pro. All number sets yielded similar line widths. The Ziegler-Nichols method was designed for a single control loop so PID1 had little effect on the signal.

## 5.2 optical pumping simulation in python

A python script was written to simulate the optical probing with 405nm light of the Optical Probing system. This code was working at a lower sophistication level but I never completed it for the full setup. I have commented it and will provide some information here in the hopes someone completes it one day. Currently the code is correct but incomplete. Here is a list of things that still need to be added.

### 5.2.1 pumping power

I left this as a undetermined coefficient for simplicity but at some point one needs to quantify how hard we are pumping. Budker has equations for this which vexed me a while. The matrix elements might not be easy to determine and need to be fitted from recorded data.

### 5.2.2 stimulated emission and excitation losses

The code is built for  $\sigma+$  transitions, and correctly adds the correct populations in each time interval. However, it assumes the losses from each hyperfine state is the same. This is not correct. A fully polarized state with not absorb  $\sigma+$  light. Initially I was doing this by hiding the polarized state but that ignores another effect. In the  $D_1$  - line different  $\sigma$  transitions have different strengths, this should be reflected in rates which states lose population. This can be implemented by simply shifting the existing exi and stim transition matrices

to be orthogonal and subtracting them from the population being targeted rather than a scalar coefficient which is currently being used.

### 5.2.3 pump detuning and power broadening

I was in the process of adding these two effects but they never put into ODE and I deleted them because they were untested and buggy. I included the code for Zeeman shifting, you need write a Voigt distribution function and add those detuning coefficients to the transitions. There will be two input parameters which are the tuned frequency of the two lasers. Power broadening can be tacked onto the Voigt distribution function I think.

### 5.2.4 $\pi$ light probing

This would be a diagonal matrix and pretty simple to implement.

### 5.2.5 Larmor precession

In principle the simulation will keep pumping forever with no restoring force. Naturally Larmor precession will restore the atom in the trap. I found this paper which has Larmor precession in their OBEs. <https://journals.aps.org/pr/abstract/10.1103/PhysRevA.63.065401>

## 5.3 possible wave plate buring

Often I found it impossible to reduce the power in the Wavemeter line to the amount one would expect to with a  $\lambda/2$  wave plate and PBS setup. Moving the  $\lambda/2$  upwards in it's mount fixed this problem temporarily and I suspect the plate is suffering from erosion under high power.

## 5.4 laser mode hopping prevention

During the F=1 scans the laser mode was always a hair away from jumping modes away from resonance. It would be prudent to tune the laser temperature to center a selected mode better with resonance to avoid this.

## 5.5 AOM scanning power shifts

For a more robust and accurate frequency lock AOM power shifts during RF scans must be mitigated. One option is a PID micro controller looking at the pass through pump beam power and controlling a variable optical retarder to maintain power throughout the scan.

## 5.6 power broadening

Measurements of resonance peaks widths were attempted to characterize the power broadening effect of pump beam power. Recorded scans were noisy and this could be revisited for greater precision.

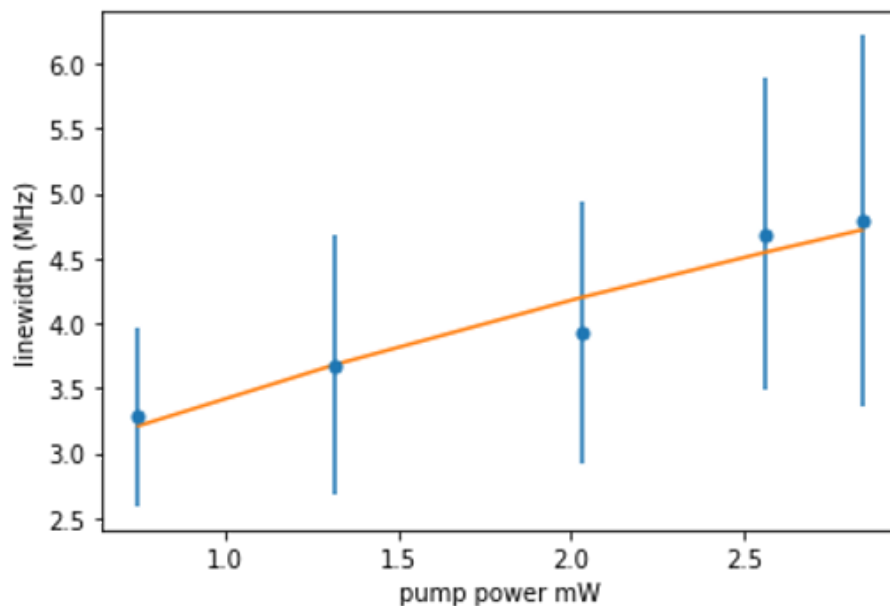


Figure 16: The power broadening observed in resonance peaks through the satSpec cell.  $\gamma_0$  was determined to be 2.5 with low accuracy seen by the large error bars.

## 6 Bibliography

### References

- [1] *Zeeman effect*. Nov. 2021. URL: [https://en.wikipedia.org/wiki/Zeeman\\_effect](https://en.wikipedia.org/wiki/Zeeman_effect).

I wasn't able to track down a paper that derived the matrix terms. It's conceivable the author derived it themselves on Wikipedia. I think the results are fairly self-evident.